Remote Sens. **2013**, *5*, 5064-5088; doi:10.3390/rs5105064

OPEN ACCESS

Remote Sensing

ISSN 2072-4292

www.mdpi.com/journal/remotesensing

Article

Assessing Water Stress of Desert Tamarugo Trees Using *in situ* Data and Very High Spatial Resolution Remote Sensing

Roberto O. Chávez [1,*], Jan G. P. W. Clevers [1], Martin Herold [1], Edmundo Acevedo [2] and Mauricio Ortiz [2,3]

[1] Laboratory of Geo-Information Science and Remote Sensing, Wageningen University, P.O. Box 47, 6700 AA Wageningen, The Netherlands; E-Mails: jan.clevers@wur.nl (J.G.P.W.C.); martin.herold@wur.nl (M.H.)

[2] Laboratorio de Relación Suelo-Agua-Planta, Facultad de Ciencias Agronómicas, Universidad de Chile, Casilla 1004, Santiago, Chile; E-Mail: eacevedo@u.uchile.cl (E.A.); mortiz@ceaf.cl (M.O.)

[3] Centro de Estudios Avanzados en Fruticultura (CEAF), Conicyt-Regional R08I1001, Av. Salamanca s/n, Rengo, Chile

* Author to whom correspondence should be addressed; E-Mails: roberto.chavez@wur.nl or roberto.chavez.o@gmail.com; Tel.: +31-317-481-552; Fax: +31-317-419-000.

Received: 24 July 2013; in revised form: 12 September 2013 / Accepted: 9 October 2013 / Published: 15 October 2013

Abstract: The hyper-arid Atacama Desert is one of the most extreme environments for life and only few species have evolved to survive its aridness. One such species is the tree *Prosopis tamarugo* Phil. Because Tamarugo completely depends on groundwater, it is being threatened by the high water demand from the Chilean mining industry and the human consumption. In this paper, we identified the most important biophysical variables to assess the water status of Tamarugo trees and tested the potential of WorldView2 satellite images to retrieve these variables. We propose green canopy fraction (GCF) and green drip line leaf area index ($DLLAI_{green}$) as best variables and a value of 0.25 GCF as a critical threshold for Tamarugo survival. Using the WorldView2 spectral bands and an object-based image analysis, we showed that the NDVI and the Red-edge Chlorophyll Index ($CI_{Red\text{-}edge}$) have good potential to retrieve GCF and $DLLAI_{green}$. The NDVI performed best for $DLLAI_{green}$ (RMSE = 0.4) while the $CI_{Red\text{-}edge}$ was best for GCF (RMSE = 0.1). However, both indices were affected by Tamarugo leaf movements (leaves avoid facing direct solar radiation at the hottest time of the day). Thus, monitoring systems

based on these indices should consider the time of the day and the season of the year at which the satellite images are acquired.

Keywords: arid ecosystems; water stress; groundwater depletion; LAI; green canopy fraction; satellite images; vegetation indices; pulvinar movement

1. Introduction

The conservation of arid vegetation is difficult to address by managers and policy makers since vegetation dots (trees and shrubs) or patches (small grasslands or limited groups of shrubs and trees) are frequently immersed into a large matrix of bare land. Therefore, its identification and assessment is costly and hard to implement. Furthermore, these dots are always closely related to the few water sources that are also required by industry and human consumption [1]. This dependency makes arid plant species susceptible to water stress although they are well adapted to survive water scarcity. Even the most resistant plant has limits, and thresholds for environmentally safe operations need to be determined in order to preserve the vegetation in deserts.

The new generation of very high spatial resolution (VHSR) satellites, starting with IKONOS in 1999 and followed by QuickBird2 in 2001, GeoEye1 in 2008 and WorldView2 in 2009, has become a real option to approach the problem of assessing the water condition of desert vegetation. Satellite images from these sensors allow identification of small dots such as individual trees, shrubs or small grass patches [2]. Since vegetation structure and composition of most arid regions is rather simple, the identification of vegetation objects using high spatial resolution remote sensing has been carried out successfully [3–5]. Nevertheless, the estimation of biophysical properties such as canopy water content, chlorophyll content or leaf area index for small vegetation objects has not been sufficiently studied yet due to the limited spectral information of VHSR satellites [6,7]. These sensors typically have only three bands in the visible region and one band in the near infra-red region (IKONOS, QuickBird2 and Geo-Eye). This spectral constraint has changed since 2009, when the WorldView2 satellite was launched, providing VHSR images with six bands in the visible region and two bands in the near infra-red region. In the near future (2014), the WorldView3 will provide images with the same eight bands of WorldView2 plus eight additional bands in the short-wave-infra-red region, opening new opportunities for the retrieval of biophysical properties of small desert features [8].

Besides spatial and spectral constraints, the assessment of arid vegetation has also temporal constraints. Desert species have developed different adaptations to cope with water scarcity and these adaptations can affect remote sensing based retrievals of biophysical parameters. A good example is the Tamarugo tree in the Atacama Desert (Northern Chile), which adjusts the leaf angle to avoid facing direct solar radiation at the hottest time of the day (midday) [8]. These leaf movements, known as pulvinar movements, are controlled by changes in cellular turgor pressure of a structure located in the base of the leaves and folioles (the pulvinus) [9], and they can have an important impact on canopy spectral reflectance [8,10,11]. Furthermore, in a previous study we analyzed the effects of water stress on Tamarugo plants under laboratory conditions by measuring a set of biophysical variables as well as the spectral reflectance response [8]. Using a modeling approach (SLC radiative transfer model [12]),

we found that the indices to retrieve canopy water content were more affected by leaf movements than those used to retrieve leaf area index (LAI). Good estimators of LAI were the Red-Edge Chlorophyll Index and the NDVI. However, our previous study [8] was conducted under laboratory conditions and no research has been carried out to test these vegetation indices under field conditions, where the solar angle and intensity are changing during the day.

In this paper, we measured and analyzed a complete dataset of biophysical and structural variables of Tamarugo trees as well as their canopy spectral reflectance response under different field conditions and water stress scenarios. Furthermore, we studied the suitability of using an up-to-date VHSR satellite image (WorldView2) to retrieve biophysical parameters of single Tamarugo trees, considering the spatial, spectral and temporal constraints previously discussed. Water condition assessment of the Tamarugo forest is urgently needed since this endemic species is currently threatened by groundwater extraction [13,14]. The Tamarugo forest is practically the only ecosystem of the Absolute Desert eco-region in Northern Chile [15,16]. It sustains a biodiversity of about 10 plant species and 30 animal species [17], some of which are endemic for the Atacama Desert (e.g., the bird *C. tamarugense* [18] and the reptile *M. theresioides* [19]). The Pampa del Tamarugal (local name of the Tamarugo forest) is distributed into two hydrological systems: Pampa del Tamarugal basin and Llamara basin (Figure 1). The most important one is the Pampa del Tamarugal basin, comprising all the plantations at the Zapiga, Pintados and Bellavista salt flats, and one small sector with natural forest (Pintados), all of which have been officially protected since 1987, and which constitute the Pampa del Tamarugal National Reserve. The second hydrological system is the Llamara basin, enclosing a well preserved natural forest located at the Llamara salt flat, which is not under official protection.

The Atacama Desert is rich in mineral resources such as copper and lithium and the mining sector is by far the most important one for the Chilean economy. Mining has created a lot of pressure to extract groundwater not only to provide drinking water to workers and the population nearby, but also as input to many industrial processes [14,20]. Currently the water extraction at the Pampa del Tamarugal basin is twice as large as natural recharges, causing a progressive groundwater depletion [13]. The Llamara basin was not exploited until 2006, when the Chilean environmental agencies (DGA and SEIA) authorized water extraction up to a maximum of 120 L/s. A new extraction up to 244 L/s was authorized on October 2011.

Chilean environmental agencies, the academic world and the private sector have extensively debated about how to define groundwater extraction thresholds to preserve the Tamarugo forest. To achieve this, a clear understanding of the relationship between the extraction rates and the water condition of the trees needs to be established. In this paper, we focus on the first part of this relationship, *i.e.*, the assessment of the water condition of the Tamarugo trees. The study of the effects of groundwater depletion (or depth) on the water status of Tamarugo at a large scale (basin) will be matter for further research. Currently, the water condition of Tamarugo trees is assessed using qualitative descriptors and an expert-knowledge approach. Several industrial projects in the area have to report about the Tamarugo forest to continue their operations. For this reason, quantitative and reliable estimations of the Tamarugo forest status are needed for water management and environmental monitoring. In order to provide such estimations, in this paper we aim specifically to:

1. Test the water stress indicators proposed by Chávez *et al.* [8] for Tamarugo plants under laboratory conditions, namely canopy water content and leaf area index, on single Tamarugo trees under different field water stress scenarios.
2. Test the vegetation indices proposed by Chávez *et al.* [8] to assess water condition of single Tamarugo trees by using the spectral bands of WorldView2 images and *in situ* measurements.
3. Study Tamarugo leaf movements during the day in the field and their implications for remote sensing based estimations of water stress.

2. Material and Methods

2.1. Species Description

The genus *Prosopis* belongs to the family Leguminoseae, subfamily Mimosaceae and comprises 44 species [21]. As other species of this genus, Tamarugo (*Prosopis tamarugo* Phil.) shows a variety of shapes and sizes, depending on genetics and growing conditions. They can reach up to 25 m height, 2 m stem diameter and 20 m crown diameter [22,23]. Tamarugos are thorny phreatophytic trees, often multi-stem, with a semi-circular crown and branches reaching the ground [22]. It is a semi-deciduous species with a vegetative period covering the whole year and a peak occurring between September and December [24,25].

2.2. Study Area

In this study, we considered two sampling sites and two field campaigns as shown in Table 1. In the first campaign (summer 2011), we measured foliar and canopy properties of 32 Tamarugo trees at two sampling sites (Figure 1): 16 trees in the natural forest located in the northern part of the Llamara basin and 16 trees in the Pintados plantation near the center of the Pampa del Tamarugal basin. Basins' borders depicted in Figure 1 were obtained from DICTUC [26]). During the second campaign (summer 2012), we studied Tamarugo leaf movements and their potential effect on the canopy spectral signature and on vegetation indices for three trees in the Llamara site. Details of the two field campaigns are given in Section 2.4. A description of the two sampling sites is given as follows.

Table 1. Field campaigns and WorldView2 images used in this study.

Field Campaign/ WorldView2 Image	Variables	Sample and Location	Dates
Field campaign summer 2011	Hydraulic, biochemical and structural variables	32 trees (16 Llamara, 16 Pintados)	24–28/01/2011
	Canopy spectral reflectance at midday (FieldSpec)	32 trees (16 Llamara, 16 Pintados) × 4 quarters per tree = 128 measurements	24–28/01/2011
Field campaign summer 2012	Diurnal leaf movements and canopy spectral reflectance (FieldSpec)	3 trees (Llamara)	13–15/01/2012
WorldView2 image winter 2011	Top-of-atmosphere (TOA) spectral reflectance	1 scene (Pintados)	13/07/2011
WorldView2 image spring 2011	Top-of-atmosphere (TOA) spectral reflectance	1 scene (Llamara)	25/09/2011

Figure 1. Satellite image (Landsat mosaic, USGS) of Pampa del Tamarugal in the Atacama Desert, Chile. Asterisks show the two sampling sites in the Pintados plantation and Llamara natural forest.

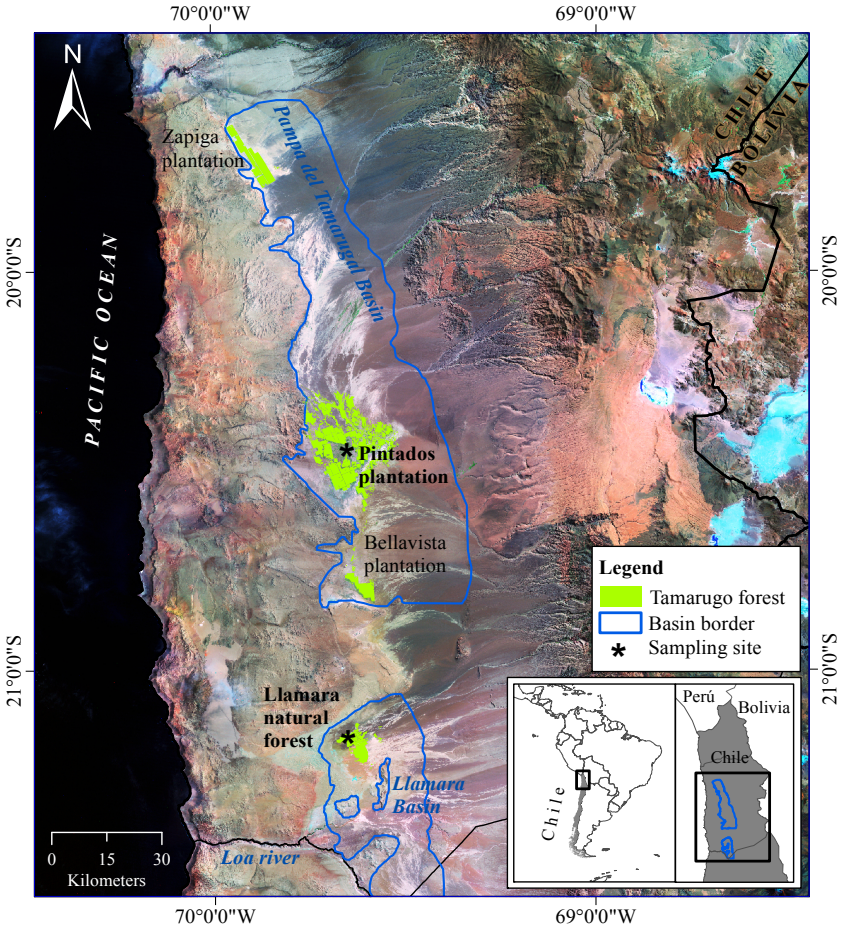

2.2.1. Llamara Site

In the Llamara forest, all trees are native, sparsely distributed (isolated trees or small groups) and at an advanced growing stage (adult or senescent trees) since regeneration is almost absent. A pumping station, operating since 2006, is located at the basin's north border. The tree sampling was performed on a north-south linear transect going from trees close to the pumping station towards the south. Since trees close to the pumping station were sparse, we selected all the available trees on the transect (eight in total). Towards the south and after a gap with no trees, we selected eight more trees on the transect from an area with more abundant trees. This way we completed a sample along the whole groundwater depletion gradient in the Llamara basin, with trees close to the pumping area facing a depletion of around 6–7 m after five years of pumping whereas trees 1500 m or more away were facing little or null depletion (Figure 2). This sample of 16 trees is part of an environmental monitoring system operated in the Llamara basin and its relevance lies in the fact that *in situ* groundwater data are provided on a monthly basis [27]. Groundwater and ground level depicted in Figure 2 were obtained from Geohidrología-SQM [27].

Figure 2. Vertical profile showing the distance of the Tamarugo trees from the extraction wells in the Llamara forest and ground water level in 2005 (before extraction), 2008 and 2011. Pictures of representative trees (A19, A20, A29 and A43) are provided in Figure 5.

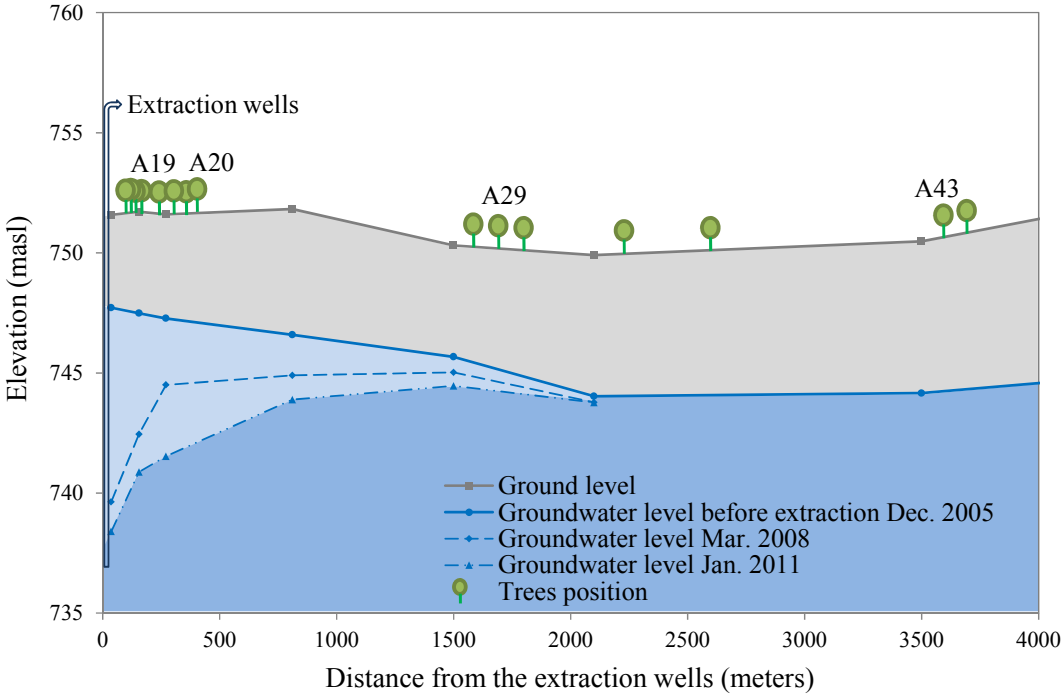

2.2.2. Pintados Site

The plantation stands in Pintados were established between 1969 and 1973 [17]. Monitoring of groundwater depletion started in the 1980s and has currently reached all plantation sectors in the Pampa del Tamarugal basin [13]. At the sampling site, the depth of the groundwater table was about 9 m in 1986 and the total depletion for the period 1986–2006 was estimated at 1.1 m [26]. The sampled trees were selected from contiguous plantation lines in a matrix of 12 × 12 m. Despite having the same groundwater depletion regimen, they visually showed a wide range in tree condition with one tree totally dry and the rest with different levels of water stress. The trees had a similar height (7 m) and about the same age (around 40 years old).

2.3. Groundwater Depletion Scenarios

In this study, we aim to find suitable remote sensing methods to estimate the water condition of Tamarugo trees for a wide range of field situations. To achieve this, we selected trees under different groundwater depletion regimens and origins (natural forest and plantations). We classified the trees as follows:

1. *Null water depletion (Dep1-null):* trees located in the Llamara site at a distance >1500 m from the pumping area (nine trees). Ground water depth was between 5 and 6 m in January 2011 (Figure 2).

2. *Short-term intensive water depletion (Dep2-int)*: trees located at the Llamara site at a distance <500 m from the pumping area with depletions of around 6–7 m in five years (seven trees). Ground water depth was between 10 and 12 m in January 2011 (Figure 2).
3. *Long-term gradual water depletion (Dep3-grad)*: trees located at the Pintados site with depletions of around 1 meter in 20 years (16 trees). At this site groundwater depth was about 11 m in 2011 according to the records of the closest DGA (Chilean Water Service) monitoring well (about 1 km away from this site).

2.4. In Situ *Measurements*

In the first field campaign (summer 2011), we studied foliar and canopy variables of Tamarugo trees growing under the three groundwater depletion scenarios (Section 2.3) and considering three levels of information: (1) hydraulic, to study the actual water supply at the root system (predawn water potential); (2) biochemical, to study effects at leaf level in terms of foliar water loss and pigment degradation; and (3) structural, to study effects at the canopy level in terms of green foliage loss. Details of the procedures and sampling schemes are given in Table 2.

For each tree, the crown was divided in four quarters following the cardinal points. Hydraulic and biochemical variables were sampled in green branches, one branch per quarter. Thus, four samples per tree were taken in the case of fully green trees. We measured predawn leaf water potential (closed stomata) using a Scholander chamber [28,29] and collected leaf samples for laboratory determinations of equivalent water thickness (EWT), chlorophyll (a + b) and carotenoids. Chlorophyll and carotenoids were determined spectrophotometrically [30]. Canopy water content (CWC) was calculated as EWT*$DLLAI_{green}$. For more details refer to Table 2.

Structural information at the canopy level was quantified by the drip line leaf area index (DLLAI), the green canopy fraction (GCF) and the combination of these two variables. First, a visual estimation of the GCF of each tree was carried out in the field (GCF_{vis}) using five categories: 0.0, 0.01–0.25, 0.25–0.50, 0.50–0.75 and 0.75–1.0. We also performed estimations of GCF from digital pictures (GCF_{pics}) taken from the four cardinal points at a fixed 10 meter distance from the tree. To do this, we developed an object based algorithm using the eCognition software to first segment the digital pictures into small tree-objects, and secondly to classify the tree-objects into brown canopy and green canopy (Figure 3B). To classify the segments we used the green ratio and red ratio calculated by rationing the red, green and blue bands of the digital pictures as shown in Table 2. Only the two pictures with full solar illumination were considered. Finally, the GCF_{pics} of each tree was obtained from the simple average of the partial results.

DLLAI was measured using a LI-COR LAI-2000 instrument (Figure 3A), which derives these quantities from gap fraction measurements. Gap fraction is the fraction of solar radiation which is not blocked by foliage and reaches the ground, in other words it is the amount of 'blue sky' that the sensor "sees" from beneath the canopy [31–33]. The sensor has a hemispherical lens, which records blue radiation under diffuse illumination conditions at five distinct angular intervals, with central zenith angles of 7, 23, 38, 53 and 68° (Figure 3A). Gap fraction is obtained by rationing a below canopy and an above canopy reading. All blocking elements are considered in the gap fraction reading, thus the instrument does not discriminate between green and brown foliage.

Table 2. Hydraulic, biochemical and structural variables measured for the 32 Tamarugo trees between 24 and 28 January 2011.

Variables	Units	Sampling Time	Sampling Scheme	Instrument/Procedure	Reference/Formula
Hydraulic					
Leaf water potential	MPa	Predawn	4 twigs per tree	Scholander chamber	[28,29]
Foliar biochemistry					
Equivalent water thickness (EWT)	g/cm^2	Midday	4 twigs per tree	Precision weight (0.0001 g) and oven	$EWT=\frac{\text{fresh leaf weight-dry leaf wei}}{\text{fresh leaf area}}$
Canopy water content (CWC)	g/cm^2				$CWC = EWT \times DLLAI_{green}$
Chlorophyll (a + b) and Carotenoids	$\mu g/cm^2$	Midday	4 twigs per tree	Spectro-photometric analysis of extracts dissolved in 80% acetone	[30]
Canopy structure					
Green canopy fraction visual estimation(GCF_{vis})		Any time	2 times, 2 surveyors	Visual estimation, using five categories: 0; 0.01–0.25; 0.25–0.50; 0.50–0.75; 0.75–1.0	$GCFvis=\frac{\text{vol. green canopy}}{\text{vol. total canopy}}$
Green canopy fraction from digital pictures (GCF_{pics})		Any time	2 digital color pictures (RGB) per tree	Object-based image analysis. Segmentation: multiresolution (scale: 10, shape: 0.5, compactness: 0.1). Classification: objects with [G/(R + G + B) > 0.34] as green canopy; objects with [R/(R + G + B) > 0.37] as brown canopy.	$GCFpics=\frac{\text{Green canopy}}{\text{(Green+Brown canopy)}}$
Drip line leaf area index (DLLAI) (green + brown)	m^2/m^2	Dawn or sunset	4 partial records (at each tree quarters)	LI-COR LAI-2000 instrument. Measurements corrected by the tree profile	$DLLAI=\frac{\text{leaf area}}{\text{drip line area}}$ [31,32,33]
Green drip line leaf area index ($DLLAI_{green}$)	m^2/m^2				$DLLAIgreen = DLLAI \times GCFpics$

One of the assumptions of the LI-COR instrument is that vegetation has a homogeneous height, which is not correct in the case of individual trees. Nevertheless, it is possible to derive the correct LAI for single trees by correcting the LI-COR readings for the tree profile (Figure 3A), obtaining as a result DLLAI, which is the LAI for the projected (to the ground) crown area or drip line area. Partial path lengths at the five angles of the LI-COR instrument were recalculated from the vertical profile of the tree on digital pictures as shown in Figure 3A. Partial DLLAI values were taken at the four quarters of

the trees by covering the hemispherical lens with a 270° cap. The final DLLAI value of each tree was obtained from the average of the partial values weighted by their partial crown volumes. Partial crown volumes were calculated internally by the LI-COR software using the corrected path lengths (Figure 3A). Because the LI-COR instrument provides values of DLLAI considering brown and green material, we multiply the DLLAI of each tree with the green canopy factor obtained from digital pictures (GCF_{pics}) obtaining as a result $DLLAI_{green}$.

Figure 3. (**A**) Procedure for measuring DLLAI of a Tamarugo tree using the LI-COR instrument. Path lengths at the five viewing angles of the instrument were corrected by the tree profile. (**B**) GCF_{pics} was estimated from digital pictures using object-based image analysis.

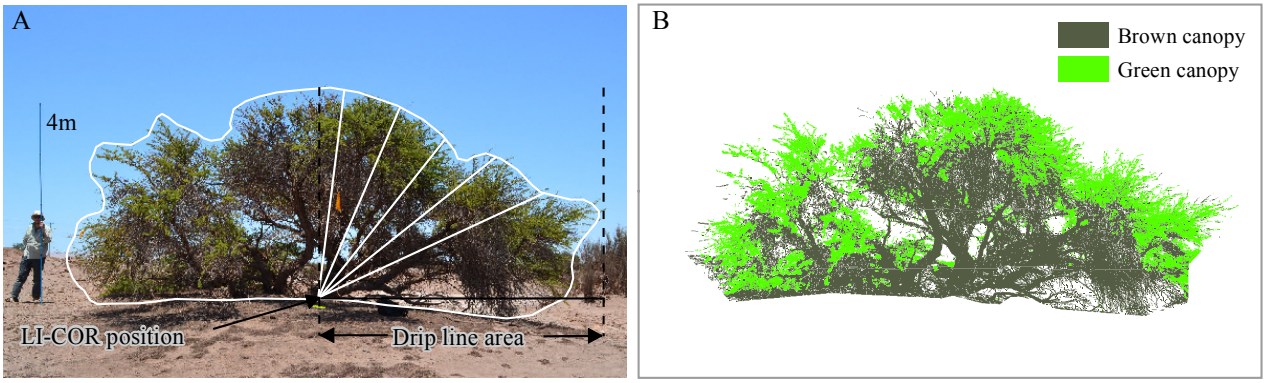

During the timeframe of performing the hydraulic, biochemical and structural sampling, we also measured the canopy spectral reflectance at the same four points of the crown for all 32 trees. We measured spectral signatures in the 400–1,300 nm range with a spectroradiometer instrument (ASD FieldSpec Pro) and using a foreoptic with instantaneous field of view (IFOV) of 25° placed in nadir position 30 cm above the canopy. We sampled reachable parts of the canopy at the same four quarters where the hydraulic and biochemical measurements were carried out. The spectral measurements were performed at 13.00 h ± 1 h. White reference measurements (spectralon) were used to calibrate the ASD instrument before every canopy reflectance measurement.

In the second field campaign (summer 2012), we studied diurnal leaf movements of three Tamarugo trees on three consecutive days in the Llamara natural forest. These leaf movements were originally reported by Chávez *et al.* [8] under laboratory conditions and showed an important effect on the canopy spectral reflectance of small Tamarugo plants. In this study, we registered diurnal leaf movements of the Tamarugo trees using a digital camera mounted on a tripod and measured canopy spectral reflectance with the FieldSpec instrument simultaneously. To perform the spectral measurements, we set the spectroradiometer instrument in nadir position 30 cm above the top of the canopy (TOC) of the Tamarugo trees. Since the solar angle changes during the day, a strict TOC position for the FieldSpec instrument is needed to minimize internal shadowing within the IFOV. Most trees are too tall to perform such measurements, and for this reason we searched for trees partially covered by sand-dunes, which allowed reaching the TOC position with a tripod. Only three trees with the above-mentioned condition were found and measured. Measurements were performed on an hourly basis from 9:00 to 18:00 hours and only interrupted at 13.00 when the instrument was shadowing the sampling area and occasionally during sand-storms.

2.5. Calculation of Spectral Vegetation Indices using Object-Based Analysis and WorldView2 Images

2.5.1. The WorldView2 Sensor

Before the WorldView2 satellite was launched in 2009, the available VHSR imagery was limited to four broad spectral bands, typically blue (450–520 nm), green (520–600 nm), red (630–690 nm) and NIR (760–900 nm) at spatial resolution of 4 m (IKONOS) to 2.4 m (QuickBird2). The WorldView2 sensor incorporated four extra bands: coastal (401–453 nm), yellow (589–627 nm), red-edge (704–744 nm) and NIR2 (862–954) and slightly modified the bands blue (448–508 nm), green (511–581 nm) and NIR (772–890 nm), which, combined with an increased spatial resolution of 0.5 m for the panchromatic channel and 2 m for the multispectral channels, enables spectral analysis of spatial features at a very high spatial resolution. In this study, we used two WorldView2 scenes to assess water stress of Tamarugo trees: the first, acquired on 13 July 2011, is covering the plantation stand of Pintados (16 trees) and the second, acquired on 25 September 2011, is covering the natural forest of Llamara (16 trees). The catalogue of WorldView2 is limited to a restricted number of dates and areas and we selected the ones closest to the field campaign date (January 2011).

The date difference between the fieldwork and the satellite image acquisitions constitutes a limitation to this study. It is a problem that users usually face when using VHSR imagery since the image catalogues are limited and ordering specific acquisition dates is very expensive. Nevertheless, Tamarugo has a vegetative period covering the whole year with a partial recession occurring between May and August and a new regrowth starting in September [34]. In other words, the trees remain green during the year and we do not expect a big seasonal effect. In order to check for this time difference, we compared the spectral vegetation indices obtained from the FieldSpec measurements (January) and the satellite images (July and September, respectively) in Section 3 and discussed our findings in Section 4.

2.5.2. Crown Delineation

Crown area was automatically delineated on the WorldView2 panchromatic images and cross-checked with *in situ* measurements of crown diameter performed at two azimuthal positions (N-S and E-W). We used a simple quad-tree object-based segmentation and classification of the mean object values in the panchromatic band (Figure 4). The algorithm was implemented in the eCognition-Developer 8TM software and it produced polygons for the crown area of all 32 single trees. Shadows next to the trees were present only in the scene acquired in winter (Figure 4B) and were manually subtracted considering the crown diameters measured in the field.

2.5.3. Vegetation Indices

We calculated the average top of atmosphere (TOA) reflectance of the pixels located inside the crown polygons for each of the eight bands of the WorldView2 multispectral image. To obtain TOA reflectance (per band), we converted the digital numbers of the original spectral bands into TOA spectral reflectance by using the absolute calibration factors as well as the solar and sensor geometry given with the scene (for details see [35]). Finally, we used the TOA reflectance values to calculate the Normalized Difference Vegetation Index (NDVI) [36] and Red-edge Chlorophyll Index ($CI_{Red\text{-}edge}$) [37] as shown in Table 3.

The selection of these indices was based on the results obtained by Chávez *et al.* [8] and the best target field indicators found in this study (GCF and $DLLAI_{green}$).

Figure 4. WorldView2 satellite images of the two sampling sites: (**A**) Llamara natural forest and (**B**) Pintados plantation. Delineated in yellow the crown of the trees identified using object-based image analysis.

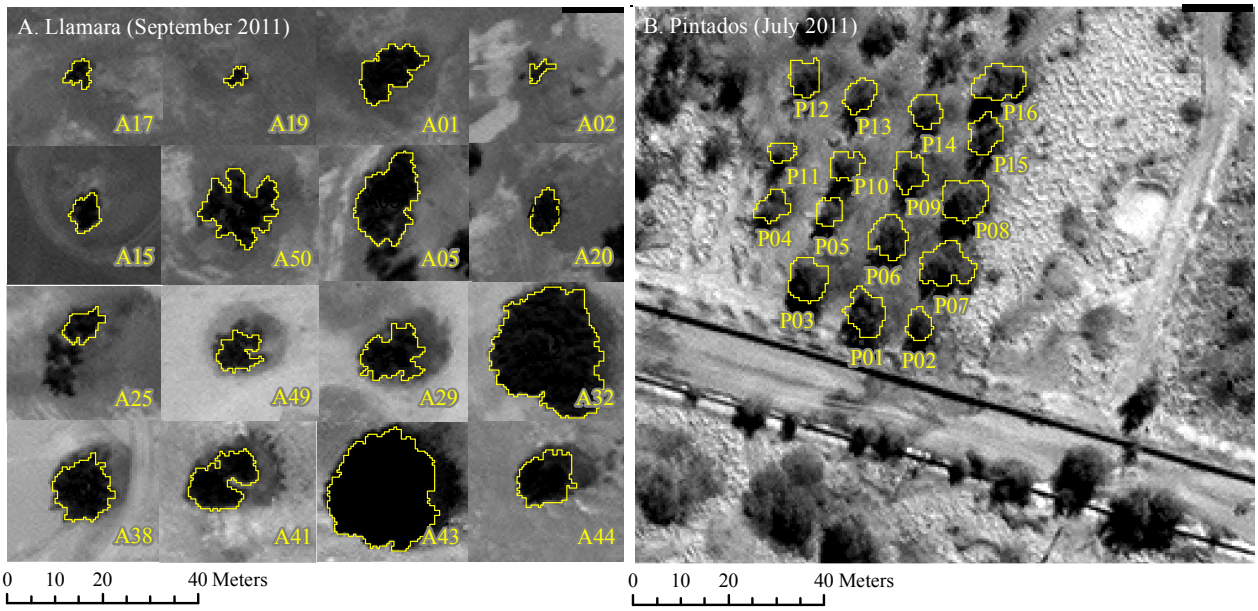

Table 3. Remote sensing vegetation indices used to estimate GCF_{pics} and $DLLAI_{green}$ of single Tamarugo trees.

Remote Sensing Feature	Formula Using the Position of the WorldView2 Spectral Bands (nm)
Normalized Difference Vegetation Index (NDVI) [36]	$(R_{831} - R_{659})/(R_{831} + R_{659})$
Red-edge Chlorophyll Index ($CI_{Red\text{-}edge}$) [37]	$R_{831}/R_{724} - 1$

2.6. Data Analysis

In order to meet the three specific objectives defined in Section 1, we performed the following data analysis:

Objective 1. Test the variables CWC and LAI as water stress indicators for single Tamarugo trees under different field water stress scenarios. We tested first for significant differences in predawn water potential between trees under the three depletion scenarios to check if they were facing different levels of water stress. Then we tested for significant differences in selected foliar and canopy variables between trees under different depletion scenarios. Additionally, we analyzed whether trees with a different GCF_{vis} were significantly different in terms of predawn water potential, foliar biochemistry and other canopy variables. Significance was tested with the Tukey-Kramer multiple comparison test for unbalanced samples with a significance level α of 0.05.

Objective 2. Test the $CI_{Red\text{-}edge}$ and NDVI to assess water condition of single Tamarugo trees by using WorldView2 images and *in situ* measurements. We tested the capability of these two vegetation

indices as best field water stress indicators using the root mean squared errors (RMSE) between estimated values and the *in situ* measurements. We compared the fitted curves and RMSE for the indices calculated using FieldSpec data, which were obtained during the field campaign, and the indices calculated from satellite data to check for seasonal effects in the remote sensing estimations.

Objective 3. Study Tamarugo leaf movements during the day in the field and their implications for remote sensing based estimations of water stress. The photographic recording of diurnal leaf movements was carried out simultaneously with the FieldSpec measurements, and therefore, diurnal changes in canopy reflection can be associated to these movements. Using the hourly FieldSpec data, we obtained hourly values of $CI_{Red\text{-}edge}$ and NDVI and calculated the correlation coefficient (R) between these values and hourly values of solar radiation. We hypothesize that solar radiation is the main environmental variable driving the leaf movements of Tamarugo trees since this has been shown for other Leguminosae plants [38–40]. Solar radiation data were obtained from the meteorological station Canchones of the Universidad Arturo Prat (20°26′36″S, 69°41′43″W). A potential correlation between spectral vegetation indices and solar radiation would imply that not only diurnal but also seasonal changes of this variable would have an impact on biophysical retrievals from remote sensing data. This is especially relevant for hyper-arid ecosystems such as the Atacama Desert, where the solar radiation can be extremely high with high fluctuations between summer and winter [41,42].

3. Results

3.1. Biophysical Response of the Tamarugo Trees under Different Water Depletion Scenarios

In the previous study of Chávez *et al.* [8], best indicators of induced water stress on small Tamarugo plants were LAI and canopy water content (CWC). This laboratory experiment also showed that leaf pigments concentrations did not change during the 15 days that plants were deprived from water. In this paper, we study whether these conclusions are also valid for adult trees in the field and under different depletion scenarios.

3.1.1. Differences between Depletion Scenarios

According to the visual assessment of green canopy fraction (GCF_{vis}), all trees with *null groundwater depletion (Dep1-null)* corresponded to the class 0.75–1.0 GCF_{vis} (see trees A43 and A29 in Figure 5 for examples). For the *short-term intensive depletion* scenario *(Dep2-int)*, five out of eight trees corresponded to the class 0.50–0.75 (see trees A19 and A20 in Figure 5 for examples), two trees belonged to 0.25–0.50 and one to 0.75–1.0. Finally, trees under *long-term gradual depletion (Dep3-grad)* corresponded to different GCF_{vis} classes (see Figure 6 for examples), where the class 0.01–0.25 was the most represented with six trees and one tree was completely dry (0.0 GCF_{vis}). The other classes were represented by three trees each. The result of this assessment indicated that the effects of groundwater depletion on foliage loss were more severe in Scenario 3 than in Scenario 2 despite the similar final water depth (about 11 m).

Table 4 shows the mean values and standard deviations of the quantitative variables measured for Tamarugo trees in the three depletion scenarios. Significant differences between mean values of the scenarios are indicated.

Figure 5. Examples of Tamarugo trees at the Llamara site. Tamarugos are sorted according to the proximity to the pumping area (left one, the closest).

Figure 6. Tamarugo trees at the Pintados site sorted by GCF_{vis}. From left to right: 0, 0.01–0.25, 0.25–0.50, 0.50–0.75 and 0.75–1.0.

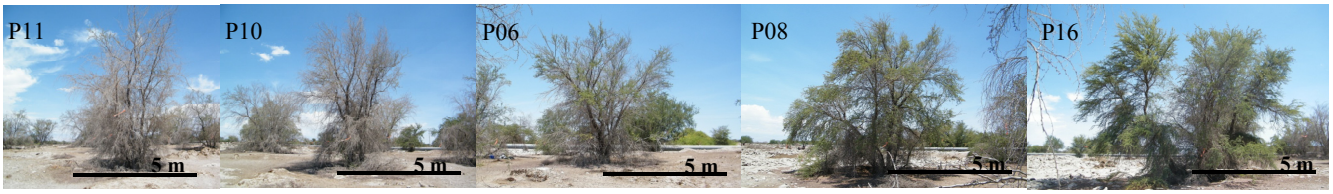

Table 4. Means and standard deviations (in brackets) of the hydraulic, biochemical and structural variables for Tamarugo trees under different groundwater depletion scenarios.

Variables	Depletion Scenarios		
	Dep1-Null	**Dep2-Intensive** (6–7 m in 5 years)	**Dep3-Gradual** (1 m in 20 years)
Hydraulic			
Predawn leaf water potential (MPa)	−2.061 (0.199) [a]	−2.194 (0.164) [a]	−2.588 (0.316) [b]
Biochemistry			
EWT (g/cm^2)	0.021 (0.002) [a]	0.019 (0.002) [b]	0.018 (0.002) [b]
Chlorophyll (a + b) ($\mu g/cm^2$)	12.28 (4.08) [a]	18.55 (2.05) [a/b]	19.23 (7.31) [b]
Carotenoids ($\mu g/cm^2$)	475.9 (115.9) [a]	620.7 (46.5) [a/b]	761.7 (236.8) [b]
Structure			
DLLAI (m^2/m^2)	2.486 (0.718) [a]	1.482 (0.664) [b]	1.658 (0.677) [b]
GCF_{pics}	0.755 (0.064) [a]	0.517(0.086) [b]	0.405 (0.253) [b]
$DLLAI_{green}$	1.887 (0.576) [a]	0.743 (0.286) [b]	0.797 (0.671) [b]
Crown area (m^2)	200.7 (175.0) [a]	69.6 (65.2) [b]	46.0 (17.13) [b]

Note: Mean values with different letters (a, b) are significantly different ($\alpha = 0.05$) according to the Tukey–Kramer multiple comparison test (after ANOVA).

Pre-dawn water potential was significantly lower for trees under long-term gradual depletion (Dep3-grad), implying that the water surrounding the root system was less available for these trees [43–45], and consequently, they were facing higher water stress than Dep1-null and Dep2-int. Additionally, the biochemical analysis showed that only trees with no groundwater depletion (Dep1-null) had higher values of EWT than trees under Dep2-int and Dep3-grad. Trees with no water depletion (Dep1-null) showed higher concentrations than Dep2-int and Dep3-grad in terms of foliar pigments (chlorophyll and carotenoids), but only Dep1-null and Dep3-grad were significantly different. At the crown level, trees under Dep2-int and Dep3-grad showed a significantly lower

DLLAI, GCF_{pics} and $DLLAI_{green}$ than trees with no ground water depletion (Dep1-null). Overall, we observed significant differences between depletion scenarios Dep1-null and Dep3-grad for all measured variables. These differences suggest that the duration of the depletion (20 years for Dep3-grad *versus* five years for Dep2-int) had a higher impact on the Tamarugo water status than the intensity of the depletion (1 meter for Dep3-grad *versus* 6–7 m for Dep2-int).

3.1.2. Differences between GCF_{vis} Classes

In addition to sharing equal depletion conditions, trees under the Dep3-grad scenario had large differences in GCF_{vis} (Figure 6). Thus, not all trees reacted equally to long-term groundwater depletion. The GCF_{vis} class of 0.01–0.25 constituted a critical threshold for the water status of Tamarugo trees, since these trees showed significantly lower values of predawn water potential (the actual direct measure of water stress) in comparison to trees of higher GCF_{vis} classes (Figure 7A). Therefore, this variable (GCF) and this threshold (<0.25) were related to high water stress.

Figure 7. Box plots of different hydraulic, biochemical and structural variables measured for the 32 Tamarugo trees grouped by GCF_{vis}: (**A**) predawn water potential, (**B**) EWT, (**C**) chlorophyll (a + b), (**D**) GCF_{pics}, (**E**) DLLAI, and (**F**) $DLLAI_{green}$.

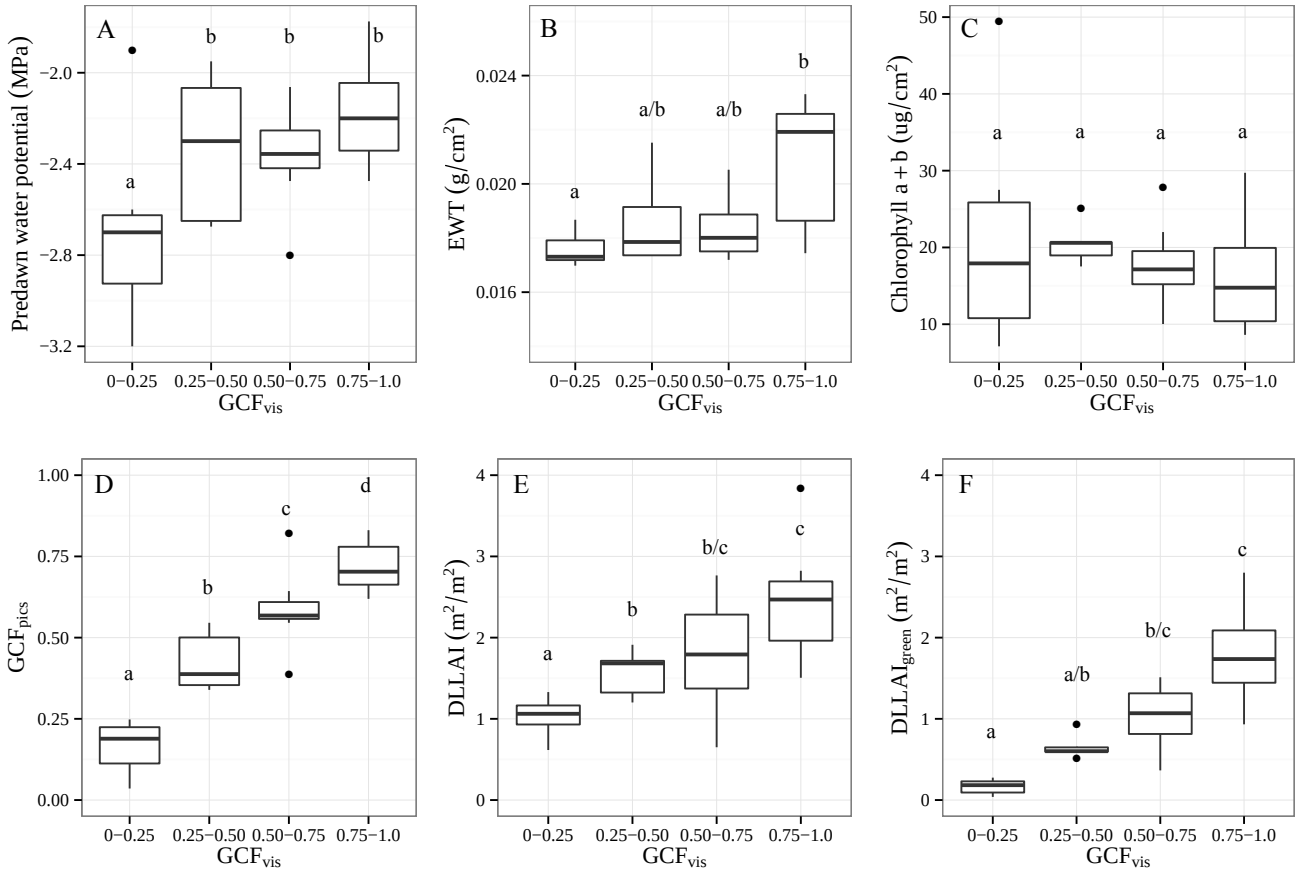

Note: Mean values with different letters are significantly different (α = 0.05) according to the Tukey–Kramer multiple comparison test (after ANOVA).

Although results showed that foliar biochemical variables as well as crown area did not significantly differ for the different green GCF_{vis} categories, the variables GCF_{pics}, DLLAI and $DLLAI_{green}$ showed significant differences as well as a positive correlation with GCF_{vis} (Figure 7). In the case of EWT, only trees at the extreme GCF_{vis} classes (0.01–0.25 and 0.75–1.0) showed significant differences. For this reason, canopy water content (CWC = EWT × LAI) estimations depended more on the LAI factor, which is $DLLAI_{green}$ in the case of individual trees.

3.2. Remote Sensing Based Estimations of Tamarugo Water Status

In the previous section, we showed that the structural variables GCF, DLLAI, and $DLLAI_{green}$ were good field indicators of the Tamarugo water status at tree level. Thus, in this section we present our findings on the suitability to use the WorldView2 spatial and spectral characteristics to retrieve these variables for single Tamarugo trees. First, we analyzed the spectral signature of trees with different GCF, and second, we studied the relationship between vegetation indices (NDVI and $CI_{Red\text{-}edge}$) and GCF and $DLLAI_{green}$, considering the spectral bands of the WorldView2 sensor. We focus our analysis on $DLLAI_{green}$ since DLLAI considers the brown and green elements of the canopy, but water stress had an impact only on the green fraction of the canopy.

Figure 8. Canopy spectral signature (average) of the 32 Tamarugo trees grouped by GCF_{vis} measured on 24–28 January 2011. The 50% band pass of the WorldView2 red, red-edge and NIR1 spectral bands are displayed as reference.

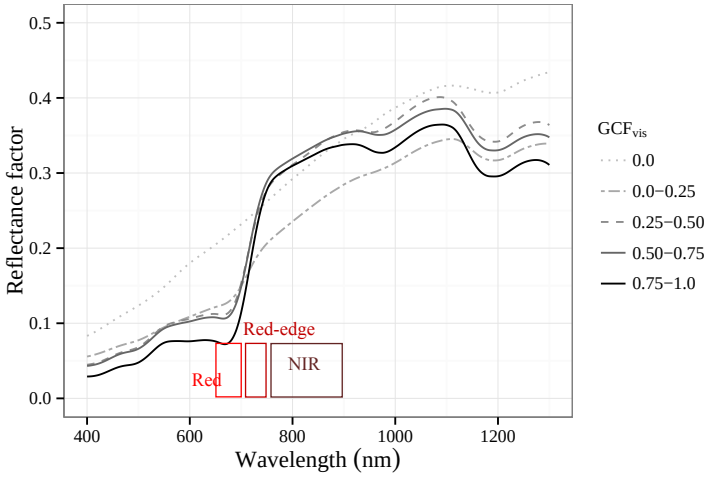

3.2.1. Spectral Response to Green Foliage Loss

Figure 8 shows the average canopy spectral signatures of the 32 Tamarugo trees grouped in five classes of green canopy fraction (GCF_{vis}) as measured with the FieldSpec instrument. From this figure, we can observe that reflectance over the near-infrared (NIR) region (760–900 nm) was higher for trees with a GCF_{vis} of 0.50–0.75 than for the trees with values of 0.75–1.0. Trees with GCF_{vis} of 0.25–0.50 showed a lower reflectance in the NIR than trees with a GCF_{vis} larger than 0.5, showing a spectral signature similar to a dead tree (GCF_{vis} = 0.0), where the brown material (branches and trunk) is dominant. In the visible region (400–700 nm) we observed similar changes to the ones observed in the

NIR region, although reflectance values for trees with GCF_{vis} values of 0.75–1.0 were always reflecting less (or absorbing more) radiation than the other trees. Another interesting spectral feature useful for water stress detection is the red-edge [46,47], which is the sharp slope of the vegetation spectral signature at 680–750 nm (Figure 8). Studies have shown that foliage loss cause the red-edge to shift towards shorter wavelengths, a phenomenon also known as "blue shift" [46–49]. In the case of Tamarugo trees the "blue shift" is not (visually) clear when comparing trees with different GCF_{vis} (Figure 8), although between the GCF_{vis} classes 0.75–1.0 and 0.50–075 the shift is slightly noticeable.

3.2.2. Vegetation Indices for GCF and $DLLAI_{green}$ Estimations

3.2.2.1. Normalized Difference Vegetation Index (NDVI)

In the previous section, we showed that the reflectance difference between the NIR and visible region decreased when trees get dry. This is clearly noticeable in Figure 9A, where the NDVI is displayed for trees with different GCF_{pics} and $DLLAI_{green}$ values. Figure 9A shows the NDVI calculated using the narrow bands of the FieldSpec instrument (1 nm band width) at the wavelengths defined in literature, *i.e.*, 670 nm for the red band and 780 nm for the NIR band [36], while Figure 9B shows the NDVI calculated using the FieldSpec bands at 659 nm and 831 nm, wavelengths where the WorldView2 red and NIR1 spectral bands are centered (see Figure 8 for a reference). Despite this shift in the spectral position, the R^2 for the linear relationship between NDVI and GCF_{pics} was high in both cases (0.80 and 0.78, respectively) and the RMSE similar (0.10 and 0.11, respectively). Moreover, the relationship between NDVI and $DLLAI_{green}$ was asymptotic, showing a lower sensitivity of NDVI for high values of DLLAI and similar RMSE values when using the spectral position defined in literature (Figure 9D) and the WorldView2 bands position (Figure 9E) with values of 0.35 and 0.36, respectively.

Figure 9C shows the relationship between NDVI and GCF_{pics} with NDVI values calculated using the broad bands of the WorldView2. In this case, the Red and NIR values were obtained by averaging the spectral values of the pixels inside the canopy polygons of each tree in the WorldView2 images (Figure 4). The NDVI values calculated this way were twice as small as values calculated using FieldSpec data. This can be explained because the FieldSpec data relate to reflectance measurements at the branch level, whereas reflectances derived from WorldView2 data relate to the canopy level. Clumping effects and internal shadowing inside the tree canopy cause lower NDVI values at the canopy level [50,51]. In spite of this, NDVI was linearly correlated to GCF showing an R^2 of 0.7 and a RMSE of 0.12. The relationship between NDVI-WV2 and DLLAI was more linear than between NDVI-FieldSpec and DLLAI, but the RMSE increased from 0.36 to 0.40 (Figure 9F). Besides the differences between the acquisition date of the images covering scenarios Dep1-null/Dep2-int (September 2011), Dep3-grad (July 2011) and the FieldSpec measurements (January 2011), the R^2 and RMSE for the relationship between NDVI-GCF using FieldSpec data (Figure 9B) was similar to the relationship GCF-NDVI using WorldView2 data (Figure 9C). For the NDVI-$DLLAI_{green}$ relationship, the RMSE was higher when using WorldView2 data (Figure 9F) than when using FieldSpec data (Figure 9E), which can be attributed to the different acquisition dates.

Figure 9. Relationships between NDVI *vs.* GCF_{pics} (**A**–**C**) and NDVI *vs.* $DLLAI_{green}$ (**D**–**F**) for 32 Tamarugo trees. NDVI was calculated using specific FieldSpec bands (first two columns) and the WorldView2 broad bands (third column).

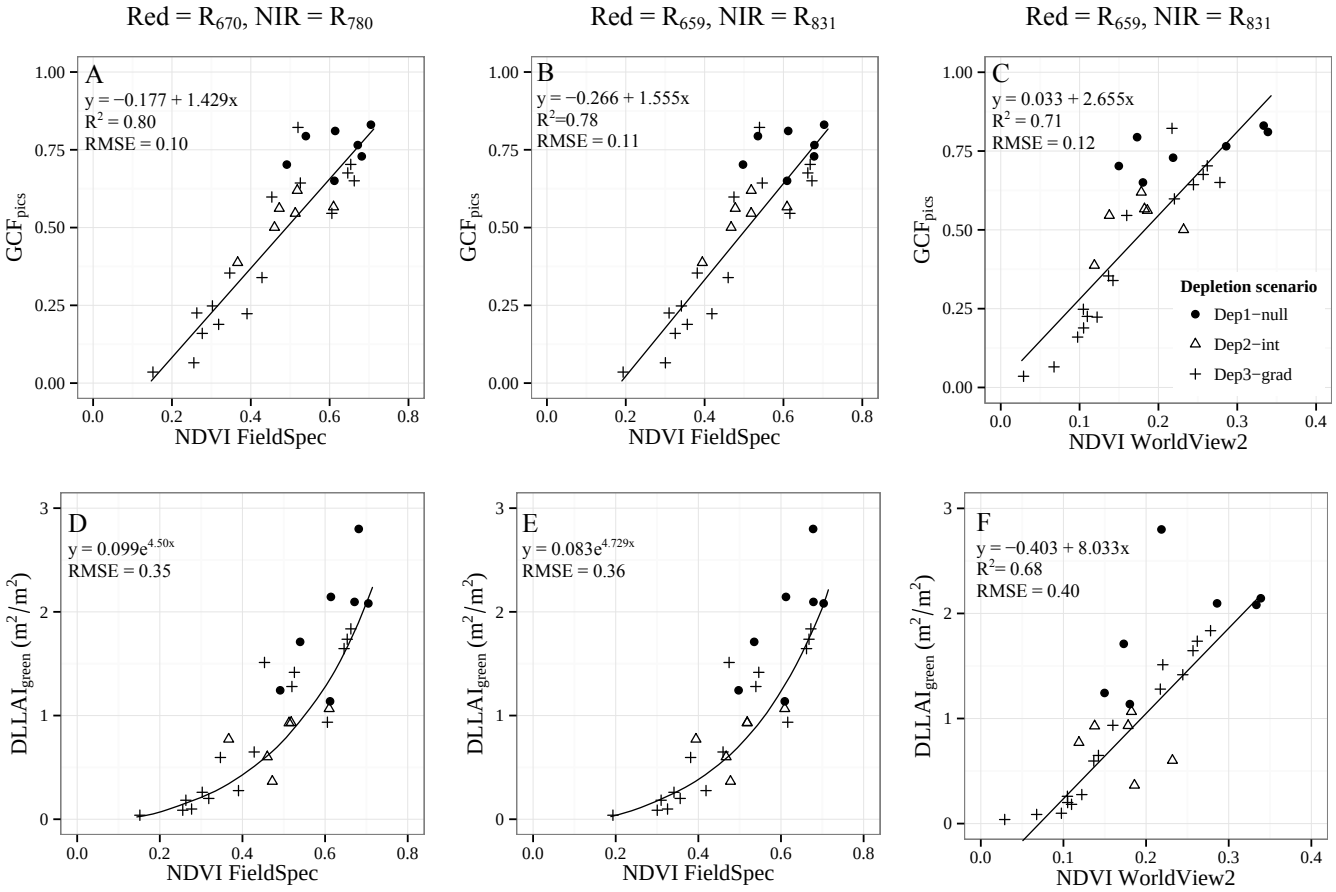

3.2.2.2. Red-edge Chlorophyll Index ($CI_{Red\text{-}edge}$)

The relationship between the $CI_{Red\text{-}edge}$ and GCF was asymptotic with a lower sensitivity for low GCF values and a RMSE of 0.1 (Figure 10A). On the contrary, the $CI_{Red\text{-}edge}$-$DLLAI_{green}$ relationship was linear with an R^2 of 0.72 and a RMSE of 0.38. However, in both cases the RMSE values increased when changing from the wavelengths defined in literature (670 nm for the red band and 710 nm for the red-edge band [37]) to the positions where the red and red-edge bands of the WorldView2 sensor are centered (659 nm and 724 nm, respectively). The $CI_{Red\text{-}edge}$ showed similar RMSE as NDVI for retrieving GCF (0.1) and an asymptotic relationship when using the wavelengths from literature, but this is not the case anymore when using the spectral band positions of WorldView2 (Figure 10B).

When using the broad bands of the WorldView2 sensor (Figure 10C), the relationship turns into asymptotic again and the RMSE was comparable to the one observed for FieldSpec data at the wavelengths suggested in literature. For $DLLAI_{green}$ estimations using the $CI_{Red\text{-}edge}$ and the WorldView2 sensor, the RMSE (0.46) was between the value observed for FieldSpec data using literature band positions (0.38) and using the WorldView2 band positions (0.52). Differences between the WorldView2 image acquisition dates and the FieldSpec measurements seem to have little effect on the R^2 and RMSE for the $CI_{Red\text{-}edge}$-GCF relationship (Figure 9B1 and 9B3), while for the

$CI_{Red\text{-}edge}$–$DLLAI_{green}$ relationship the RMSE increased when using WorldView2 data (Figures 10D and 10F). Overall, the NDVI constituted the best estimator for $DLLAI_{green}$ while the $CI_{Red\text{-}edge}$ was the best for estimating GCF for tree objects extracted from WorldView2 imagery.

Figure 10. Relationships between $CI_{Red\text{-}edge}$ *vs.* GCF_{pics} (**A**–**C**) and $CI_{Red\text{-}edge}$ *vs.* $DLLAI_{green}$ (**D**–**F**) for 32 Tamarugo trees. $CI_{Red\text{-}edge}$ was calculated using specific FieldSpec bands (first two columns) and the WorldView2 broad bands (third column).

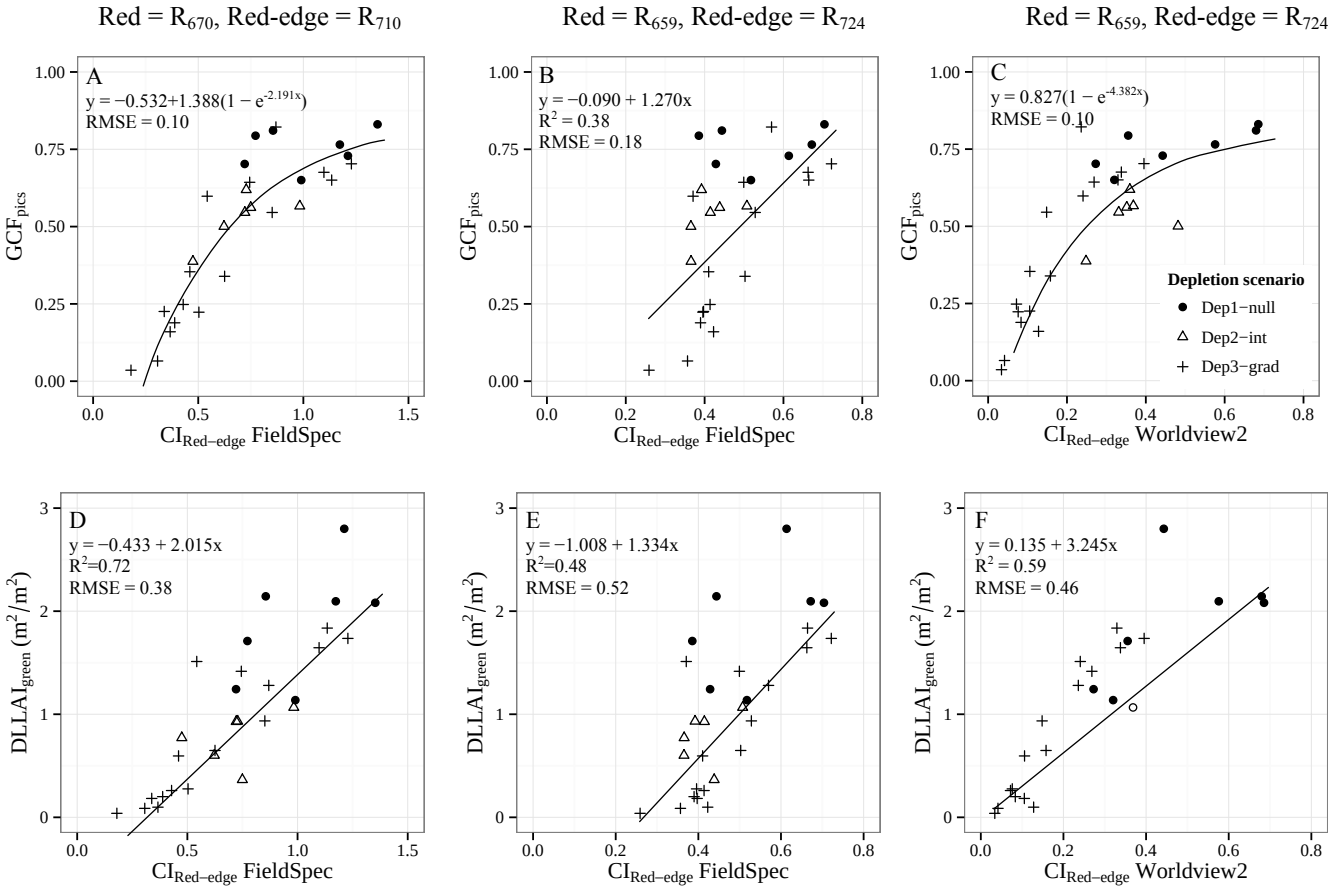

3.3. Effects of Tamarugo Pulvinar Movements on Spectral Reflectance

Figure 11 shows pulvinar movements of Tamarugo trees under field conditions and Figure 12A shows the canopy spectral reflectance changes throughout the day. From 9.00 hours onwards leaves were changing gradually from a planophile leaf distribution (parallel to the leveled horizon) to a more erectophile distribution (perpendicular to the leveled horizon), making canopy reflectance to drop during the day. In Figure 12B, we depicted the NDVI and $CI_{Red\text{-}edge}$ as well as solar radiation recorded hourly during three days of the summer 2012 campaign. Both indices were calculated using FieldSpec 1 nm bands at the wavelengths where the WorldView2 bands are centered. This figure shows that the lowest values for both vegetation indices were around 13.00 h when the solar radiation was reaching its maximum. The correlation coefficient (R) between NDVI and solar radiation was negative and higher (R = −0.52) than in case of the R between $CI_{Red\text{-}edge}$ and solar radiation (R = −0.24).

Figure 11. Pulvinar movement of Tamarugo leaves recorded on 13 January 2012.

Figure 12. (**A**) Hourly changes on Tamarugo canopy spectral signature measured on 13 January 2012 (summer). (**B**) Hourly values of NDVI and $CI_{Red\text{-}edge}$ (FieldSpec data) for three Tamarugo trees and solar radiation measured on three consecutive days: 13–15 January 2012.

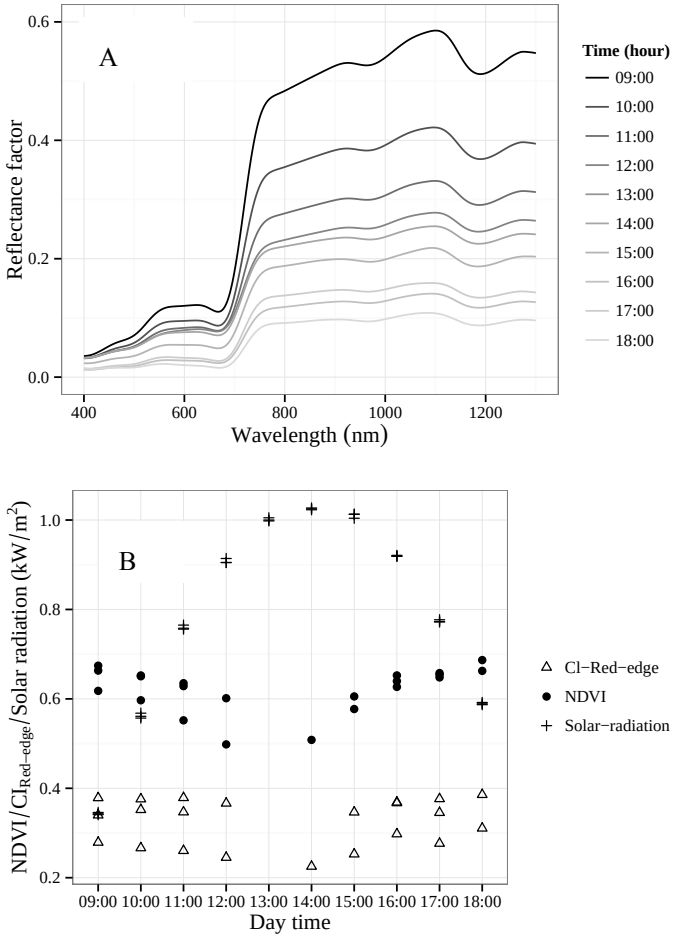

4. Discussion

The analysis of the biophysical variables of trees under different depletion scenarios in this study showed no clear trends (Table 4). Scenarios Dep2-int and Dep3-grad did not show significant differences for the biochemical and structural variables, although trees for Dep3-grad were facing a higher water stress (as shown by the predawn leaf water potential). Besides, trees sharing equal depletion conditions reacted differently to changes in groundwater supply. This is well illustrated in Figure 6, where we can observe trees for scenario Dep3-grad with large differences in GCF_{vis}. This variability in the response of Tamarugo to water stress implies that water extraction on a large scale may not affect the Tamarugo population homogeneously in space, and therefore, an assessment of water condition at the tree level is necessary to understand the impact of groundwater extraction.

Although a clear trend in the biophysical variables for the three depletion scenarios was absent, we observed significant differences between the null depletion scenario and the two water stress scenarios for the biochemical and structural variables (Table 4), which means that trees under water stress had (a) lower water concentration, (b) higher pigment concentration, and (c) lower green foliage fraction. Another interesting finding from Table 4 is that Dep3-grad may induce higher water stress than Dep2-int. In other words, Tamarugo trees would be more sensitive to the duration of the water stress rather than to the intensity of the water stress. However, this hypothesis needs to be tested using more trees and more information on the groundwater depth and depletion for the whole aquifer. The goal of the current study was not to estimate the extent of the water depletion or different levels of depletion, but to define useful indicators for tree condition and to test whether remote sensing based indices can be used to estimate these indicators. Therefore, potential autocorrelation of trees within one depletion scenario may exist, but no conclusions on the depletion scenarios themselves have been made.

After studying differences in the biophysical variables for different water scenarios, we analyzed trees with different green canopy fraction, that was visually assessed (GCF_{vis}). Although Tamarugo trees are defined as semi-deciduous species [24,25,34], healthy trees look green during the whole year and this is the reason why current water condition assessments use GCF_{vis} estimations. When grouping the 32 trees into four categories of GCF_{vis}, we found that trees with 0.01–0.25 GCF_{vis} presented a significantly lower predawn water potential than trees from the other three higher GCF_{vis} classes, which means that Tamarugo is able to keep its water status at normal ranges till losing about 75% of green foliage. This value (GCF = 0.25) is therefore critical for Tamarugo's water balance and can be used as a threshold for conservation purposes. Furthermore, we did not observe significant differences between the GCF_{vis} classes for the foliar biochemical variables, except for EWT and only when comparing the 0.01–0.25 and 0.75–1.0 classes. This is an indication that Tamarugo trees cope with water stress by adjusting their water balance at the canopy level rather than adjusting their foliage properties. This is in line with research conducted by Asner *et al.* [6] in the Chihuahuan desert (New Mexico) where they found that foliar spectral properties of desert plants were very stable along environmental gradients in comparison with canopy variables, which were very variable.

In this study, we implemented a quantitative method to estimate the green canopy fraction of single Tamarugo trees using digital pictures (GCF_{pics}), which showed a good correspondence with the visual method GCF_{vis} (Figure 7D). This quantitative approach, based on segmentation of the digital pictures using the red-green-blue (RGB) bands has been successfully used before for retrieving the green

fraction of crops [52,53]. The use of the green ratio and red ratio to discriminate green and brown segments of the trees within the pictures allowed us to use images with different illumination conditions and with different radiometric resolutions (different cameras), providing an observer-independent indicator of water stress. GCF_{pics} can be used for assessing green foliage loss for single trees regardless of the tree size. This variable is also easy to interpret for policy makers since it gives a direct value of the percentage of the remaining foliage. If the purpose of the assessment is to study the effects of groundwater depletion on the biomass of Tamarugo trees, $DLLAI_{green}$ is more suitable than GCF since it gives a quantitative estimation of the amount of green material available.

WorldView2 satellite imagery provided a unique source of detailed spatial and spectral data, allowing single tree identification and calculation of the NDVI and the $CI_{Red\text{-}edge}$ per tree. Our results showed that both indices provided accurate estimations of GCF and $DLLAI_{green}$ for single Tamarugo trees. These results demonstrate that an assessment of the condition of single Tamarugo trees is possible at a regional scale, and therefore, a digital inventory and assessment will be the logical next step.

To perform such an assessment, temporal constraints must be taken into account since we have shown that the spectral reflectance varied during the day due to Tamarugo leaf movements. These movements constitute an adaptation of Tamarugo trees to survive the high solar radiation of the Atacama Desert and have an important impact on remote sensing based vegetation indices. We observed a negative correlation coefficient (R) of about −0.5 between the NDVI and solar radiation during the day, and consequently, we may expect also that NDVI values in summer could be lower than in winter only because of more solar radiation. We hypothesize that this fact could be the explanation why in Figure 9C some trees with high GCF at scenario Dep1-null had low NDVI values. The WorldView2 scene corresponding to the scenarios Dep1-null and Dep2-int was acquired in September (spring, high solar radiation), while the image corresponding to the scenario Dep3-grad was acquired in July (winter, low solar radiation). Thus, full green trees would have been able to adjust their leaf angle distribution according to the solar radiation, showing lower values of NDVI in spring. Although we cannot discard Tamarugo's phenological cycle as a cause of seasonal changes in vegetation indices, we believe that pulvinar movements play a major role. Nevertheless, this hypothesis needs to be tested in more detail and it will be subject for further research.

5. Conclusions and Recommendations

Green canopy fraction (GCF), estimated with object based image analysis on digital pictures, and green drip line leaf area index ($DLLAI_{green}$), measured with a LI-COR instrument, are good field estimators of the condition of single Tamarugo trees. We recommend using GCF for environmental monitoring and DLLAI for biomass studies. We suggest a critical GCF value of 0.25 for Tamarugo survival, below which the trees are facing leaf water potentials (predawn) significantly below normal ranges.

Single tree identification, crown size delineation and estimations of $DLLAI_{green}$ and GCF were successfully performed using WorldView2 high spatial resolution satellite images and an object based image analysis approach. This methodology constitutes a powerful tool for assessing and monitoring the effects of groundwater depletion on Tamarugo trees at a large regional scale since it copes with the spatial heterogeneity in the forest. The NDVI constituted the best estimator for $DLLAI_{green}$, while the

Red-edge Chlorophyll Index was the best one for estimating GCF for tree objects extracted from WorldView2 imagery.

Tamarugo pulvinar movements, an adaptation to survive the extreme conditions of the Atacama Desert, affected vegetation indices calculated from canopy spectral reflectance. Therefore, they can only be used for monitoring purposes if they (a) have been measured at the same time during the day and at the same season, or (b) they have been corrected for this temporal effect. No research has been carried out so far to cope with the second option and it will be subject for further research.

Acknowledgments

This work has been supported by CONICYT-Chile and Wageningen University. The authors would like to thank Digital Globe for providing the WorldView2 imagery, to CONAF-Chile and SQM-S.A. for supporting the logistics during the field campaigns, and UNAP for providing the meteorological data. Special thanks to X. Aravena (SQM), C. Squella, M. Garrido (SAP-UCH), and M. Decuyper (WUR) for assisting the harsh fieldwork.

Conflicts of Interest

The authors declare no conflict of interest.

References

1. Ezcurra, E. *Global Deserts Outlook*; United Nations Environment Programme: Nairobi, Kenya, 2006.
2. Blaschke, T. Object based image analysis for remote sensing. *ISPRS J Photogram. Remote Sens.* **2010**, *65*, 2–16.
3. Laliberte, A.S.; Rango, A.; Havstad, K.M.; Paris, J.F.; Beck, R.F.; McNeely, R.; Gonzalez, A.L. Object-oriented image analysis for mapping shrub encroachment from 1937 to 2003 in southern New Mexico. *Remote Sens. Environ.* **2004**, *93*, 198–210.
4. Laliberte, A.S.; Fredrickson, E.L.; Rango, A. Combining decision trees with hierarchical object-oriented image analysis for mapping arid rangelands. *Photogram. Eng. Remote Sens.* **2007**, *73*, 197–207.
5. Gibbes, C.; Adhikari, S.; Rostant, L.; Southworth, J.; Qiu, Y., Application of object based classification and high resolution satellite imagery for savanna ecosystem analysis. *Remote Sens.* **2010**, *2*, 2748–2772.
6. Asner, G.P.; Wessman, C.A.; Bateson, C.A.; Privette, J.L. Impact of tissue, canopy, and landscape factors on the hyperspectral reflectance variability of arid ecosystems. *Remote Sens. Environ.* **2000**, *74*, 69–84.
7. Borzuchowski, J.; Schulz, K. Retrieval of leaf area index (LAI) and soil water content (WC) using hyperspectral remote sensing under controlled glass house conditions for spring barley and sugar beet. *Remote Sens.* **2010**, *2*, 1702–1721.
8. Chávez, R.O.; Clevers, J.G.P.W.; Herold, M.; Ortiz, M.; Acevedo, E. Modelling the spectral response of the desert tree *Prosopis tamarugo* to water stress. *Int. J. Appl. Earth Obs. Geoinf.* **2013**, *21*, 53–65.

9. Taiz, L.; Zeiger, E. *Plant Physiology*; Sinauer Associates: Sunderland, MA, USA, 2010.
10. Kimes, D.S.; Kirchner, J.A. Diurnal variations of vegetation canopy structure. *Int. J. Remote Sens.* **1983**, *4*, 257–271.
11. Moran, M.S.; Pinter, P.J., Jr; Clothier, B.E.; Allen, S.G. Effect of water stress on the canopy architecture and spectral indices of irrigated alfalfa. *Remote Sens. Environ.* **1989**, *29*, 251–261.
12. Verhoef, W.; Bach, H. Coupled soil-leaf-canopy and atmosphere radiative transfer modeling to simulate hyperspectral multi-angular surface reflectance and TOA radiance data. *Remote Sens. Environ.* **2007**, *109*, 166–182.
13. Rojas, R.; Dassargues, A. Groundwater flow modelling of the regional aquifer of the Pampa del Tamarugal, Northern Chile. *Hydrogeol. J.* **2007**, *15*, 537–551.
14. Romero, H.; Méndez, M.; Smith, P. Mining development and environmental injustice in the Atacama Desert of Northern Chile. *Environ. Justice* **2012**, *5*, 70–76.
15. Gajardo, R. *La Vegetación Natural de Chile Clasificación y Distribución Geográfica*; Editorial Universitaria: Santiago, Chile, 1994.
16. CONAMA. *Biodiversidad de Chile, Patrimonio Y Desafíos*; Ocho Libros Editores: Santiago, Chile, 2008.
17. CONAF. *Plan de Manejo Reserva Nacional Pampa del Tamarugal*; Corporación Nacional Forestal (CONAF). Ministerio de Agricultura: Gobierno, Chile, 1997; p. 110.
18. Estades, C.F. Natural history and conservation status of the Tamarugo Conebill in northern Chile. *Wilson Bull.* **1996**, *108*, 268–279.
19. Ramírez-Leyton, G.; Pincheira-Donoso, D. *Fauna del Altiplano y Desierto de Atacama. Vertebrados de la Provncia de El Loa*; Phrynosaura Ediciones: Calama, Chile, 2005.
20. Oyarzún, J.; Oyarzún, R. Sustainable development threats, inter-sector conflicts and environmental policy requirements in the arid, mining rich, Northern Chile territory. *Sustain. Dev.* **2011**, *19*, 263–274.
21. Burkart, A. A monograph of the genus *Prosopis* (Leguminosae subfam. Mimosoideae). *J. Arnold. Arbor.* **1976**, *57*, 219–249.
22. Altamirano, H. *Prosopis tamarugo* Phil. Tamarugo. In *Las especies arbóreas de los bosques templados de Chile y Argentina. Autoecología*; Donoso, C., Ed.; Marisa Cuneo Ediciones: Valdivia ,Chile, 2006; pp 534–540.
23. Riedemann, P.; Aldunate, G.; Teillier, S. *Flora nativa de valor ornamental. Chile, Zona Norte. Identificación y propagación*; Productora Gráfica Andros Ltda: Santiago, Chile, 2006; p. 404.
24. Acevedo, E.; Ortiz, M.; Franck, N.; Sanguineti, P. *Relaciones hídricas de Prosopis tamarugo Phil. Uso de isótopos estables*; Universidad de Chile: Santiago, Chile, 2007; p. 82.
25. Sudzuki, F. Environmental Influence on Foliar Anatomy of *Prosopis Tamarugo* Phil. In *The Current State of Knowledge on Prosopis Tamarugo*; Habit, M., Ed.; FAO: Rome, Italy, 1985.
26. DICTUC. Anexo VIII.2 Modelación de la Evolución del Nivel de la Napa en la Pampa del Tamarugal. In *EIA proyecto Pampa Hermosa*; Dirección de Investigaciones Científicas y Tecnológicas Universidad Católica de Chile, Santiago, Chile, 2008; p 169.
27. Geohidrología-SQM. Informe Semestral 2. In *Plan de Segumiento Ambiental Hidrogeológico Proyecto Pampa Hermosa*; Geohidrología: Santiago, Chile, 2012; p. 118.

28. Meyer, W.S.; Ritchie, J.T. Resistance to water flow in the Sorghum plant. *Plant. Physiol.* **1980**, *65*, 33–39.
29. Scholander, P.F.; Hammel, H.T.; Bradstreet, E.D.; Hemmingsen, E.A. Sap pressure in vascular plants. *Science* **1965**, *148*, 339–346.
30. Lichtenthaler, H.K.; Wellburn, A.R. Determination of total carotenoids and chlorophyll a and b of leaf extract in different solvents. *Biochem. Soc. Trans.* **1983**, 591–592.
31. LI-COR. *LAI-2000 Plant Canopy Analyser. Instruction Manual*; LICOR: Lincoln, NE, USA, 1992.
32. Jonckheere, I.; Fleck, S.; Nackaerts, K.; Muys, B.; Coppin, P.; Weiss, M.; Baret, F. Review of methods for *in situ* leaf area index determination: Part I. Theories, sensors and hemispherical photography. *Agric. For. Meteorol.* **2004**, *121*, 19–35.
33. Peper, P.J.; McPherson, E.G. Evaluation of four methods for estimating leaf area of isolated trees. *Urban. For. Urban. Green.* **2003**, *2*, 19–29.
34. Ortiz, M.; Silva, P.; Acevedo, E. Leaf Water Parameters in Prosopis Tamarugo Phil. Subject to a Lowering of the Water Table. In *Nivel freático en la Pampa del Tamarugal y Crecimiento de Prosopis tamarugo Phil*; Tesis para optar al Grado Académico de Doctor en Ciencias Silvoagrpecuarias y Veterinarias: Santiago, Chile, 2010; pp. 15–42.
35. Updike, T.; Comp, C. *Radiometric Use of WorldView2 Imagery*; Technical Note; Revision 1; DigitalGlobe, Inc.: Longmont, CO, USA, 2010; p. 17.
36. Tucker, C.J. Red and photographic infrared linear combinations for monitoring vegetation. *Remote Sens. Environ.* **1979**, *8*, 127–150.
37. Gitelson, A.A.; Keydan, G.P.; Merzlyak, M.N. Three-band model for noninvasive estimation of chlorophyll, carotenoids, and anthocyanin contents in higher plant leaves. *Geophys. Res. Lett.* **2006**, *33*, L11402.
38. Pastenes, C.; Pimentel, P.; Lillo, J. Leaf movements and photoinhibition in relation to water stress in field-grown beans. *J. Exp. Bot.* **2005**, *56*, 425–433.
39. Liu, C.C.; Welham, C.V.J.; Zhang, X.Q.; Wang, R.Q. Leaflet movement of *Robinia pseudoacacia* in response to a changing light environment. *J. Integr. Plant. Biol.* **2007**, *49*, 419–424.
40. Pastenes, C.; Porter, V.; Baginsky, C.; Norton, P.; González, J. Paraheliotropism can protect water-stressed bean (*Phaseolus vulgaris* L.) plants against photoinhibition. *J. Plant. Physiol.* **2004**, *161*, 1315–1323.
41. Ortega, A.; Escobar, R.; Colle, S.; de Abreu, S.L. The state of solar energy resource assessment in Chile. *Renewable Energy* **2010**, *35*, 2514–2524.
42. Hirschmann, R.J. Records on solar radiation in Chile. *Solar Energy* **1973**, *14*, 129–138.
43. Schmidhalter, U. The gradient between pre-dawn rhizoplane and bulk soil matric potentials, and its relation to the pre-dawn root and leaf water potentials of four species. *Plant. Cell. Environ.* **1997**, *20*, 953–960.
44. Veste, M.; Staudinger, M.; Küppers, M. Spatial and temporal variability of soil water in drylands: Plant water potential as a diagnostic tool. *Forestry Studies China* **2008**, *10*, 74–80.
45. Richter, H. Water relations of plants in the field: some comments on the measurement of selected parameters. *J. Exp. Bot.* **1997**, *48*, 1–7.

46. Boochs, F.; Kupfer, G.; Dockter, K.; Kuhbauch, W. Shape of the red edge as vitality indicator for plants. *Int. J. Remote Sens.* **1990**, *11*, 1741–1753.
47. Filella, I.; Penuelas, J. The red edge position and shape as indicators of plant chlorophyll content, biomass and hydric status. *Int. J. Remote Sens.* **1994**, *15*, 1459–1470.
48. Horler, D.N.H.; Dockray, M.; Barber, J. The red edge of plant leaf reflectance. *Int. J. Remote Sens.* **1983**, *4*, 273–288.
49. Carter, G.A.; Knapp, A.K. Leaf optical properties in higher plants: linking spectral characteristics to stress and chlorophyll concentration. *Am. J. Bot.* **2001**, *88*, 677–684.
50. Malenovský, Z.; Bartholomeus, H.M.; Acerbi-Junior, F.W.; Schopfer, J.T.; Painter, T.H.; Epema, G.F.; Bregt, A.K. Scaling dimensions in spectroscopy of soil and vegetation. *Int. J. Appl. Earth Obs. Geoinf.* **2007**, *9*, 137–164.
51. Moorthy, I.; Miller, J.R.; Noland, T.L. Estimating chlorophyll concentration in conifer needles with hyperspectral data: An assessment at the needle and canopy level. *Remote Sens. Environ.* **2008**, *112*, 2824–2838.
52. Baret, F.; de Solan, B.; Lopez-Lozano, R.; Ma, K.; Weiss, M. GAI estimates of row crops from downward looking digital photos taken perpendicular to rows at 57.5° zenith angle: Theoretical considerations based on 3D architecture models and application to wheat crops. *Agric. For. Meteorol.* **2010**, *150*, 1393–1401.
53. Liu, J.; Pattey, E.; Admiral, S. Assessment of *in situ* crop LAI measurement using unidirectional view digital photography. *Agric. For. Meteorol.* **2013**, *169*, 25–34.